

6-2018

# Arthropod EVs Mediate Dengue Virus Transmission Through Interaction With a Tetraspanin Domain Containing Glycoprotein Tsp29Fb

Ashish Vora  
*Old Dominion University*

Wenshuo Zhou  
*Old Dominion University*

Berlin Londono-Renteria

Michael Woodson

Michael B. Sherman

*See next page for additional authors*

Follow this and additional works at: [https://digitalcommons.odu.edu/biology\\_fac\\_pubs](https://digitalcommons.odu.edu/biology_fac_pubs)

 Part of the [Cell Biology Commons](#), [Virology Commons](#), and the [Virus Diseases Commons](#)

## Repository Citation

Vora, Ashish; Zhou, Wenshuo; Londono-Renteria, Berlin; Woodson, Michael; Sherman, Michael B.; Collpitts, Tonya M.; Neelakanta, Girish; and Sultana, Hameeda, "Arthropod EVs Mediate Dengue Virus Transmission Through Interaction With a Tetraspanin Domain Containing Glycoprotein Tsp29Fb" (2018). *Biological Sciences Faculty Publications*. 327.  
[https://digitalcommons.odu.edu/biology\\_fac\\_pubs/327](https://digitalcommons.odu.edu/biology_fac_pubs/327)

## Original Publication Citation

Vora, A., Zhou, W., Londono-Renteria, B., Woodson, M., Sherman, M. B., Collpitts, T. M., . . . Sultana, H. (2018). Arthropod EVs mediate dengue virus transmission through interaction with a tetraspanin domain containing glycoprotein Tsp29Fb. *Proceedings of the National Academy of Sciences of the United States of America*, 115(28), E6604–E6613. doi:10.1073/pnas.1720125115

---

**Authors**

Ashish Vora, Wenshuo Zhou, Berlin Londono-Renteria, Michael Woodson, Michael B. Sherman, Tonya M. Collpitts, Girish Neelakanta, and Hameeda Sultana



# Arthropod EVs mediate dengue virus transmission through interaction with a tetraspanin domain containing glycoprotein Tsp29Fb

Ashish Vora<sup>a</sup>, Wenshuo Zhou<sup>a</sup>, Berlin Londono-Renteria<sup>b</sup>, Michael Woodson<sup>c</sup>, Michael B. Sherman<sup>c,d</sup>, Tonya M. Colpitts<sup>e,f</sup>, Girish Neelakanta<sup>a,g</sup>, and Hameeda Sultana<sup>a,g,h,1</sup>

<sup>a</sup>Department of Biological Sciences, Old Dominion University, Norfolk, VA 23529; <sup>b</sup>Department of Entomology, Kansas State University, Manhattan, KS 66506; <sup>c</sup>Department of Biochemistry and Molecular Biology, University of Texas Medical Branch, Galveston, TX 77555; <sup>d</sup>Sealy Center for Structural Biology and Molecular Biophysics, University of Texas Medical Branch, Galveston, TX 77555; <sup>e</sup>Department of Microbiology, Boston University School of Medicine, Boston University, Boston, MA 02215; <sup>f</sup>National Emerging Infectious Diseases Laboratories, Boston University, Boston, MA 02215; <sup>g</sup>Center for Molecular Medicine, Old Dominion University, Norfolk, VA 23529; and <sup>h</sup>Department of Medicine, Division of Infectious Diseases and International Health, University of Virginia School of Medicine, Charlottesville, VA 22908

Edited by Lynn Pulliam, San Francisco VA Medical Center, University of California, San Francisco, CA, and accepted by Editorial Board Member Peter Palese June 4, 2018 (received for review November 20, 2017)

Dengue virus (DENV) is a mosquito-borne flavivirus that causes dengue fever in humans, worldwide. Using *in vitro* cell lines derived from *Aedes albopictus* and *Aedes aegypti*, the primary vectors of DENV, we report that DENV2/DENV3-infected cells secrete extracellular vesicles (EVs), including exosomes, containing infectious viral RNA and proteins. A full-length DENV2 genome, detected in arthropod EVs, was infectious to naïve mosquito and mammalian cells, including human-skin keratinocytes and blood endothelial cells. Cryo-electron microscopy showed mosquito EVs with a size range from 30 to 250 nm. Treatments with RNase A, Triton X-100, and 4G2 antibody-bead binding assays showed that infectious DENV2-RNA and proteins are contained inside EVs. Viral plaque formation and dilution assays also showed securely contained infectious viral RNA and proteins in EVs are transmitted to human cells. Up-regulated HSP70 upon DENV2 infection showed no role in viral replication and transmission through EVs. In addition, qRT-PCR and immunoblotting results revealed that DENV2 up-regulates expression of a mosquito tetraspanin-domain-containing glycoprotein, designated as Tsp29Fb, in *A. aegypti* mosquitoes, cells, and EVs. RNAi-mediated silencing and antibody blocking of Tsp29Fb resulted in reduced DENV2 loads in both mosquito cells and EVs. Immunoprecipitation showed Tsp29Fb to directly interact with DENV2 E-protein. Furthermore, treatment with GW4869 (exosome-release inhibitor) affected viral burden, direct interaction of Tsp29Fb with E-protein and EV-mediated transmission of viral RNA and proteins to naïve human cells. In summary, we report a very important finding on EV-mediated transmission of DENV2 from arthropod to mammalian cells through interactions with an arthropod EVs-enriched marker Tsp29Fb.

ness (dengue fever) leads to stages of dengue hemorrhagic fever, dengue shock syndrome, multiple organ failure, and death (6–9). Recently, the WHO immunization group SAGE (Strategic Advisory Group of Experts) has recommended the use of dengue vaccine (a live attenuated tetravalent dengue vaccine CYD-TDV, named Dengvaxia) developed by Sanofi Pasteur. Apart from this partially effective vaccine, there are no drugs or pan-vaccines available for human use to prevent/cross-protect or treat dengue infections in endemic areas (8–10).

So far, no studies have elucidated whether arthropods secrete extracellular vesicles (EVs), including small vesicles referred to as exosomes, and whether pathogens are transmitted from the vector to the vertebrate host via mosquito-derived EVs. Because of the occurrence of RNA in the small EVs (11, 12), we hypothesized whether these EVs are carriers of positive-sense single-stranded RNA viruses belonging to the family Flaviviridae. Since their discovery in the early 1980s, exosomes have been recognized as small membrane-bound EVs that act as imperative intercellular messengers carrying and transporting functional RNAs, miRNA, proteins, and lipids (13–15). EVs are basically of endocytotic origins that are released from the cells upon fusion of multivesicular bodies with the cellular membranes (13–15). Recent discoveries of functional RNA and miRNA within EVs has increased the attention that has led to the emergence of numerous studies in identifying novel molecules present in the EVs (13–16). The International Society for Extracellular Vesicles defines exosomes with new nomenclature as small

arthropod EVs | dengue | transmission | HSP70 | Tsp29Fb

Arthropod-borne diseases are of major concern to mankind. Primary arthropod vectors, such as mosquitoes, transmit several pathogens, including flaviviruses that cause severe diseases in humans (1, 2). The roles of vector molecules and their mechanisms in transmission of arthropod-borne flaviviruses from vector to vertebrate host are not completely understood. Targeting essential vector molecules used by flaviviruses during transmission to the vertebrate host is envisioned as the best approach to develop therapeutics and vaccine candidates (3). Currently, there are no specific drugs/therapies or vaccines for several of these arthropod-borne flaviviral infections (4–6). Development of novel and potential approaches is essential to control flaviviral diseases. Current research efforts are focused to understand pathogenesis of the emerging mosquito-borne dengue virus (DENV; serotype 2) and its detrimental effects in causing numerous human deaths throughout the world. With regard to the global impact from arthropod-borne diseases, dengue is the most critical human arbovirus that exists as four serotypes: DENV1, -2, -3, and 4. The acute asymptomatic ill-

## Significance

So far, no studies have reported whether dengue virus uses arthropod extracellular vesicles (EVs) for its transmission from vector to the mammalian host. Our study reports a very significant finding on EV-mediated transmission of dengue viruses (serotypes 2 and 3) from mosquito to mammalian, including human cells, through interactions with an arthropod EV-enriched tetraspanin domain-containing glycoprotein, Tsp29Fb.

Author contributions: H.S. designed research; H.S. conceived, designed, and coordinated the entire study; A.V., W.Z., M.W., M.B.S., G.N., and H.S. performed research; B.L.R., T.M.C., G.N., and H.S. contributed reagents/analytic tools; A.V., W.Z., M.W., M.B.S., G.N., and H.S. analyzed data; and H.S. wrote the paper.

The authors declare no conflict of interest.

This article is a PNAS Direct Submission. L.P. is a guest editor invited by the Editorial Board.

Published under the PNAS license.

<sup>1</sup>To whom correspondence should be addressed. Email: hsltana@odu.edu.

This article contains supporting information online at [www.pnas.org/lookup/suppl/doi:10.1073/pnas.1720125115/-DCSupplemental](http://www.pnas.org/lookup/suppl/doi:10.1073/pnas.1720125115/-DCSupplemental).

Published online June 26, 2018.

extracellular vesicles of 40–120 nm; we have considered exosomes together with other sized vesicles as EVs in our analysis (17). Our findings from this current study, showing the presence of the DENV2 full-length genome and viral proteins in mosquito cell-derived EVs, provide important data for the current and future avenues in understanding biology of arthropod EVs in pathogen transmission. We also determine that arthropod HSP70 (heat-shock protein 70, a specific EV/exosomal marker in mammals) is induced in mosquito cells upon DENV2 infection, but its inhibition had no effect in blocking viral replication and transmission via EVs. In addition, identification of a tetraspanin domain-containing glycoprotein, Tsp29Fb, a putative ortholog of human CD63 (mammalian EVs/exosome marker), showed conservation in EV-mediated communication, suggesting an essential therapeutic strategy in blocking transmission of DENV2 from arthropods to humans. Collectively, this study is not only critical in understanding the molecular basis of the modes of flaviviral transmission from the arthropod vector, but may also potentially lead to the development of better strategies to interfere with the life cycle of this and perhaps other medically important vectors.

## Results

### Mosquito Cell-Derived EVs Contain DENV2 Infectious RNA and Proteins.

We used *Aedes albopictus* and *Aedes aegypti* mosquito cell lines (C6/36 and Aag-2, respectively) as a model to understand the interactions of DENV (serotype 2) with mosquito vectors. DENV2 [multiplicity of infection (MOI) 5] readily infected the C6/36 cell line with significantly ( $P < 0.05$ ) increased viremia at 72 and 96 h postinfection (hpi) in comparison with 48 hpi (SI Appendix, Fig. S1A). Next, we analyzed whether C6/36 cells secrete EVs, including small EVs, and if mosquito-borne flaviviruses use those EVs as modes of pathogen transmission. C6/36 cell-derived EVs contained DENV2 capsid mRNA loads in a time-dependent manner, with

increased viral loads at 72 hpi (MOI 5), compared with the early tested time points of 24 and 48 hpi (SI Appendix, Fig. S1B). In addition, we determined DENV2 loads in *A. aegypti* mosquitoes at different time points (24, 48, and 72 hpi) of infection (SI Appendix, Fig. S1C). Because of increased viral loads (both in cell line and in vivo), we selected 72 hpi as the time point for the isolation of EVs from mosquito cells. EVs were isolated by either a density-gradient (DG) centrifugation technique [OptiPrep (DG-EVs isolation) as described in refs. 18 and 19] or by using a commercially available exosome isolation reagent and following the manufacturer's instructions (ThermoScientific), or by differential ultracentrifugation with slight modifications and longer spin times for 155 min (SI Appendix, Fig. S2) (11, 15, 18–23). Detailed protocols for EV isolation by DG-Exo and ultracentrifugation methods are shown as schematics (SI Appendix, Fig. S2). Cryo-electron microscopy (cryo-EM) performed on C6/36 cell-derived EV fractions showed the presence of purified mosquito EVs with the size range of 30–250 nm in diameter (Fig. 1A), which are similar to EVs isolated from mammalian cells (11, 15, 18, 24–26). Quantitative analysis of the heterogeneous population of arthropod-derived EVs showed the highest percentage to be in sizes between 50 and 100 nm (in diameter) in both uninfected and DENV2-infected groups (SI Appendix, Fig. S3A and B). However, DENV2-infected cell-derived EVs had increased (50–100 nm) and decreased (100–150 nm) percentage sizes in comparison with the uninfected control (SI Appendix, Fig. S3A and B). The observation of lower percentage of larger EVs (in the size range of 200–350 nm) upon DENV2 infection in comparison with the uninfected group suggests that DENV2 may stimulate production of smaller-sized EVs (SI Appendix, Fig. S3A and B). Countings of total number of EVs from uninfected or DENV2-infected (MOI 5, 72 hpi) cryo-EM images collected from at least three independent isolations showed no significant differences (SI Appendix, Fig. S3C). Because the physical

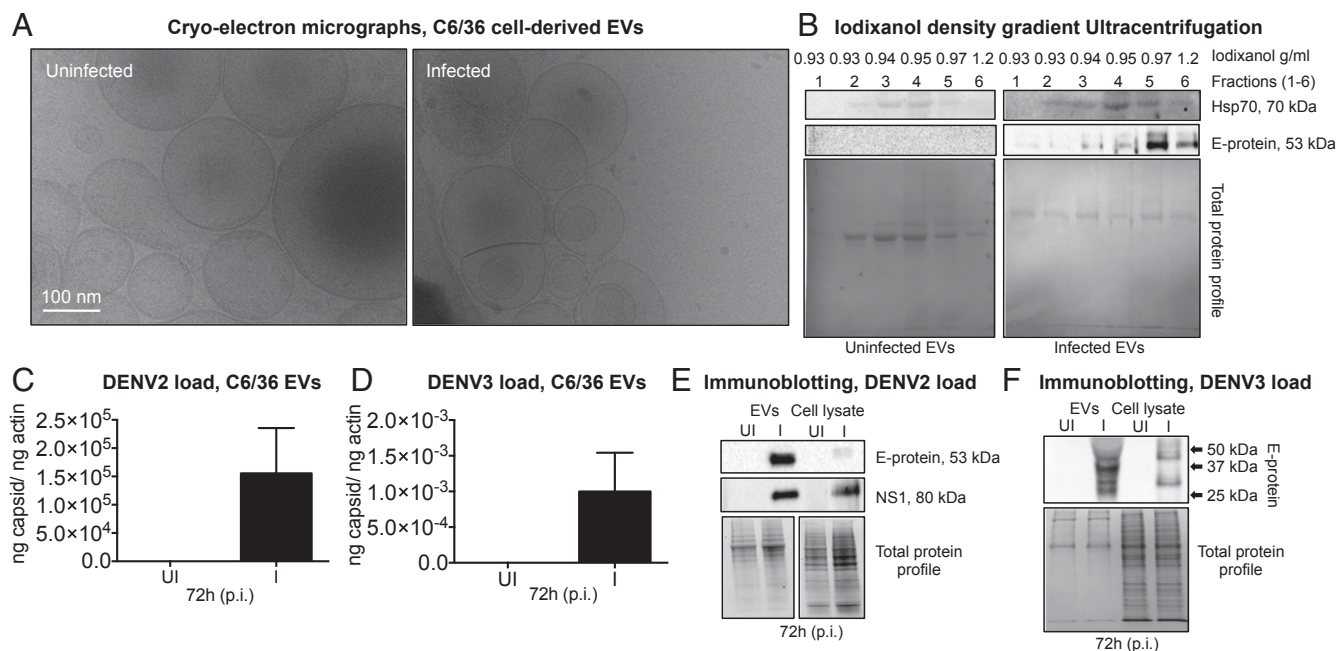


**Fig. 1.** EVs derived from mosquito cells contain DENV2/DENV3 RNA and proteins. (A) Cryo-EM images showing EVs isolated from uninfected or DENV2-infected (MOI 5, 72 hpi) C6/36 cells. [Scale bar, 100 nm (in diameter).] (B) Immunoblotting gel image from DG-EV-iso preparation showing enhanced DENV2 E-protein levels and HSP70 in fractions 4–6. EVs derived from uninfected cells serve as control. Total protein profiles from both groups are shown for comparison. Fraction number and calculated iodixanol density (g/mL) is shown for reference. qRT-PCR analysis showing DENV2 (C) or DENV3 (D) loads in EVs isolated from C6/36 cells at 72 hpi ( $n = 5$  in both panels). DENV2/DENV3 capsid mRNA levels were normalized to mosquito actin levels.  $P$  value determined by Student's two-tail  $t$  test is shown. (E) Immunoblotting analysis showing detection of DENV2 E-protein and NS1 in EV fraction and total lysates from whole cells prepared from uninfected (UI) or infected (I) C6/36 cells at 72 hpi (MOI 5). (F) DENV3-specific E-protein in EVs and total cell lysates from uninfected (UI) or infected (I) C6/36 cells at 72 hpi (MOI 5) is shown. Protein sizes are indicated as kilodaltons. Images showing total protein profiles serve as controls in both E and F.

characterization and quality of the EVs as revealed by cryo-EM imaging was very pure, we quantified the EVs through estimating total protein amounts by Bradford protein assay (BCA). EVs isolated from different numbers of plated cells ( $10^4$ ,  $10^5$ ,  $10^6$ ,  $10^7$ , and  $1 \times 10^8$ ), showed linear increase in the concentration of total EV protein (SI Appendix, Fig. S3 D and E). No differences were observed in EV total protein concentrations from DENV2-infected or uninfected controls (SI Appendix, Fig. S3 D and E). These data correlated with the observation of no differences in the total number of EVs between DENV2-infected or uninfected groups (SI Appendix, Fig. S3C). In both groups, increasing density of cells showed higher increments in total protein concentrations of EVs (SI Appendix, Fig. S3 D and E).

Next, we collected six different fractions from the DG-EV isolation method (SI Appendix, Fig. S2A). Mosquito HSP70 was detected in 20  $\mu$ L of each of the infected or uninfected EV fractions from 2 to 6, with increased levels in fraction 4 (Fig. 1B). No HSP70 was detected in fraction 1 from EVs isolated from uninfected or DENV2-infected groups (Fig. 1B). However, the level of HSP70 was found to be increased in fractions isolated from DENV2-infected EVs in comparison with the uninfected fractions that served as controls. (Fig. 1B). We found that DENV2 envelope (E)-protein (detected by highly cross-reactive 4G2 monoclonal antibody that recognizes flavivirus E-protein, both endogenous and glycosylated forms) was enhanced in infected EV fraction 5 in comparison with the other fractions (Fig. 1B). Immunoblotting also showed detection of both DENV2-glycosylated (Fig. 1B, Upper band) and endogenous (Fig. 1B, Lower band) E-protein in fraction 5. As expected, DENV2 E-protein was not detected in any uninfected controls (Fig. 1B). The Ponceau S-stained images showed total protein profile in each fraction (Fig. 1B). Density of each fraction was estimated by a control density-gradient experiment with similar volume of 0.25 M sucrose/10 mM Tris pH 7.5 that was run in parallel to determine the iodixanol concentrations. In addition, we performed DG-EV isolation by filtering the culture supernatants with 0.22- $\mu$ m filters that resulted in 12 fractions. Similar results were obtained with filtered samples, where enhanced amounts of E-protein were detected in higher density of 10, 11, and 12 EV fractions (SI Appendix, Fig. S3F). HSP70 was detected in all samples with increased amounts in fractions 10 and 11 (SI Appendix, Fig. S3F). Ponceau S-stained images showed a total protein profile in each fraction (SI Appendix, Fig. S3F).

Next, we determined if mosquito cell-derived EVs contain the full-length DENV2 genome. PCR analysis (with oligonucleotides producing overlapping amplicons covering entire DENV2 sequence) noted the presence of the full-length DENV2 genome in C6/36 cell-derived EVs (SI Appendix, Fig. S4A). Fragments 1–10 amplified products of 1,102 bp, 1,110 bp, 1,124 bp, 1,114 bp, 1,118 bp, 1,141 bp, 1,104 bp, 1,135 bp, 1,110 bp, and 1,048 bp (SI Appendix, Fig. S4A). Fragment 11 (3' end of the genome) amplified multiple products, including the expected size of 717 bp (SI Appendix, Fig. S4A). Several PCR attempts to amplify fragment 11 consistently showed an appearance of multiple bands, perhaps suggesting the loop nature of the 3' end of the genome (SI Appendix, Fig. S4A). We have been able to successfully show the presence of entire DENV2 genome inside mosquito EVs. Quantitative real-time PCR (qRT-PCR) also showed DENV2 total capsid mRNA in EVs derived from infected (MOI 5, 72 hpi) C6/36 cells (Fig. 1C). To address if other serotypes of DENV are also present and transmitted easily as being part of the EVs, we tested DENV3 viral RNA in EVs. DENV3-infected (MOI 5, 72 hpi) C6/36 cell-derived EVs also showed the presence of viral capsid mRNA, suggesting EVs as mediators of perhaps all serotypes of DENVs (Fig. 1D). In addition, DENV2 E- and nonstructural 1 (NS1) proteins were also detected in C6/36 cell lysates and EVs (Fig. 1E). It was noted that E-protein levels were enhanced in EVs in comparison with cell lysates at 72 hpi, whereas no differences were observed with

NS1 protein levels in either EVs or total cell lysates (Fig. 1E). Furthermore, we detected enhanced E-protein levels in DENV3-infected (MOI 5, 72 hpi), C6/36 cell-derived EVs in comparison with the total cell lysates (Fig. 1F). Coomassie-stained gel images show the total protein profiles in both DENV2 and DENV3 groups (Fig. 1E and F). The observation of a reduced number of protein bands in both DENV2 and DENV3 EV fractions in comparison with the whole-cell lysate fractions, respectively (Fig. 1E and F), suggests a restricted regulation, sorting, and export of proteins into mosquito EVs.

**DENV2 RNA and Proteins Are Securely Contained Inside the EVs.** To not rule out the possibility of DENV2 particles being present either inside or outside of the EVs, we performed cryo-EM analysis on C6/36 cell-derived EV fractions (six). DENV2-infected (MOI 5, 72 hpi) C6/36 cell-derived EV fractions did not show any viral particles or virions either inside or outside of these EV fractions (SI Appendix, Fig. S4B). These data suggest that viral RNA and proteins are perhaps sufficient to modulate the infection of naïve recipient cells. We also tested if viral RNA is binding to the outside of the EVs and may be then transmitted to the recipient cells. We did not find any differences in viral loads of naïve C6/36 cells upon incubation with EVs prepared from DENV2-infected (MOI 5, 72 hpi) RNaseA-treated (5  $\mu$ g/mL, for 15 min, at 37 °C) or untreated groups (SI Appendix, Fig. S5A). Naïve C6/36 cells incubated with EVs derived from uninfected cells (as independent batch), but treated with RNase A, were kept as internal control (SI Appendix, Fig. S5A). In another independent RNaseA-treatment assay, we included MOI 5 of DENV2 laboratory virus stocks [collected from 14 d post-infection (dpi) C6/36 cell culture supernatants] along with infectious EVs (collected from DENV2 infected C6/36 cells, MOI 5, 72 hpi) for comparison (SI Appendix, Fig. S5B). We obtained reproducible results with no differences in viral loads in naïve C6/36 cells upon incubation with EVs or laboratory viral stocks prepared from DENV2-infected RNaseA-treated or untreated groups (SI Appendix, Fig. S5B). Because the viral genome is deep inside and not accessible in enveloped DENV2, RNaseA treatments showed no effects. To confirm that the viral proteins too are contained inside the mosquito cell-derived EVs, and are not present in the PBS suspensions that are free or depleted of EVs, we designed and performed an E-protein 4G2-antibody bead binding assay to confirm that viral E-protein is not present outside of the EVs as a contaminant. No significant ( $P < 0.05$ ) differences were observed in viral loads between DENV2-infected (MOI 5, 72 hpi) EV fractions treated with either 4G2 antibody (that binds to viral E-protein) or with relevant isotype control antibody or the untreated controls (SI Appendix, Fig. S5C). We also tested the DENV2 laboratory stocks (MOI 5) as controls that showed reduced DENV2 loads in C6/36 cells in comparison with the isotype antibody-treated or untreated controls (SI Appendix, Fig. S5D). These data served as a positive control for the EV group. Taken together, these data suggest that E-protein is securely contained inside the arthropod EVs.

To further confirm that viral E-protein is contained inside the EVs, we performed native-PAGE followed by immunoblotting with 4G2 antibody on EV fractions (collected from DENV2-infected, MOI 5, 72 hpi cells) treated with 0.1% Triton X-100 (a detergent that lyse the EV lipid bilayer membrane) for 30 min at room temperature, or treated with freeze/thaw cycle (three rounds of freezing, for 1 h each time, at  $-80$  °C). Untreated samples (held at 4 °C) served as controls. An enhanced level of DENV2 E-protein (in native state at  $\sim$ 200–250 kDa) was detected in Triton X-100-treated EV fractions in comparison with the levels in untreated fractions (SI Appendix, Fig. S5E). The lower molecular mass of E-protein in Triton X-100-treated EV fractions indicated the lysis and separation of higher molecular structures that may exist as dimers or oligomers (SI Appendix, Fig. S5E). Ponceau S-stained images showed the total protein profile and served as control (SI Appendix, Fig. S5E). In addition, immunostaining analysis with 4G2 antibody showed that EVs treated/lysed with 0.1% of Triton X-100 had a

higher fluorescent signal for DENV2 E-protein in comparison with untreated EV fractions (*SI Appendix, Fig. S5F*). As expected, E-protein staining was enhanced upon permeabilization of EVs, suggesting the presence of E-protein inside EVs (*SI Appendix, Fig. S5F*). ELISA with 4G2 antibody further supported the native-PAGE and immunostaining analyses, where higher loads of DENV2 E-protein were detected when EVs were permeabilized with 0.1% of Triton X-100 in comparison with untreated controls (*SI Appendix, Fig. S5G*). The lysis of EV lipid-bilayer would release the viral E-protein contained inside the EVs, thereby resulting in enhanced detection of E-protein upon permeabilization with Triton X-100. Overall, these data suggest that DENV2 RNA and proteins are securely contained inside the arthropod EVs.

**DENV2 Infectious RNA and Proteins Are Transmitted to Mosquito, Murine, and Human Cells Through Arthropod EVs.** To address whether DENV2 RNA and proteins contained in mosquito cell-derived EVs are viable and capable to infect arthropod/vertebrate host cells and form infectious particles, we used EV fractions (pellet) and EV-free or EV-depleted supernatant (EDS; generated during EV pelleting and before PBS wash) (*SI Appendix, Fig. S2B*) fractions isolated from 72 hpi (MOI 5) C6/36 cells. Virus-dilution assays performed on naïve C6/36 cells with infectious EV fractions (dilution 3; 1,000-fold diluted) showed enhanced fluorescent signal for E-protein detected by 4G2 antibody in comparison with EDS-treated cells (Fig. 2A). Furthermore, EV fractions in dilution one (10-fold) showed similar enhanced fluorescence signal for E-protein in comparison with EDS fractions (*SI Appendix, Fig. S6A*). The dilutions of 10 and 1,000 correspond to 12.6  $\mu\text{g}$  and 0.126  $\mu\text{g}$  of total EVs protein, respectively, as estimated by the BCA method. These data suggest that DENV2 RNA and proteins contained inside EVs are highly infectious. In addition, infectious mosquito EV fractions and EDS were tested in plaque assays (as described in *SI Appendix, SI Materials and Methods*) to determine the infectivity and replication of viral RNA and formation of viable plaques in Vero cells. First, we determined infection kinetics (MOI 5) in Vero cells and noted that an increased peak of DENV2 infection was at 96 hpi (*SI Appendix, Fig. S6B*). Mosquito cell-derived infectious EV pellet fractions yielded plaques at dilutions of 1:10 that were too numerous to count, and around

25–30 plaques at a dilution of 1:100, and fewer than 5 plaques in dilutions of 1:1,000 (Fig. 2B). No plaques were detected in plates where Vero cells were treated with the EDS undiluted fractions collected before pelleting the EVs (Fig. 2B). Plaque assays further confirmed that mosquito cell-derived EVs contain DENV2 RNA and proteins, capable of replication and forming viable viral plaques that are highly infectious to the mammalian cells. We analyzed whether infectious mosquito EVs are capable of transmission of DENV2 to other cells. First, infection of DENV2 in several other cell lines was assessed, which showed detectable loads at 72 hpi (MOI 5) (*SI Appendix, Fig. S6 C–E*). Next, we analyzed the ability of DENV2 infectious EVs to infect naïve C6/36 cells, mouse monocyte-derived dendritic cells (Mo-DCs), human-skin keratinocytes (HaCaT cells), and human blood endothelial cells (HUVEC). Because of detectable loads of DENV2 at 72 hpi (MOI 5), we considered infecting the mammalian cells via infectious EVs collected from 72 hpi DENV2-infected (MOI 5) C6/36 cells. These infectious EVs showed the transmission and reinfection ability to infect naïve mosquito C6/36 cells, mouse Mo-DCs, HaCaT cells, and HUVEC cells (Fig. 2C). Detectable viral loads were found in all of these tested cell lines at 72 h postincubation; however, significant ( $P < 0.05$ ) DENV2 loads were noted in mouse and human cells in comparison with mosquito cells (Fig. 2C). No viral loads were detected in any tested cell lines incubated with EDS fractions (Fig. 2C). Overall, these results suggest that DENV2 viral RNA and proteins exit mosquito cells via EVs, and that these infectious EVs mediate transmission of DENVs to human cells.

**Role of Mosquito HSP70 in EV-Mediated DENV2 Transmission.** This intracellular molecular chaperone, required for protection and recovery from stress, is secreted via unknown exocytotic pathways and trafficked into EVs (27, 28). HSP70 has also been identified and characterized from *A. aegypti* and *A. albopictus* mosquitoes (29, 30). Our study demonstrated that arthropod HSP70 is present in EVs derived from mosquito cells. To understand the importance of HSP70 in mosquito EVs and DENV2 transmission, we investigated the role of two isoforms of *hsp70* genes (GenBank accession nos. JN132154 and XM\_019672019) present in the *A. albopictus* genome. qRT-PCR analysis revealed that both *hsp70* isoforms were up-regulated in C6/36 cells upon DENV2 infection (MOI 5) at 48 h and 72 hpi in comparison with 24 hpi and uninfected controls

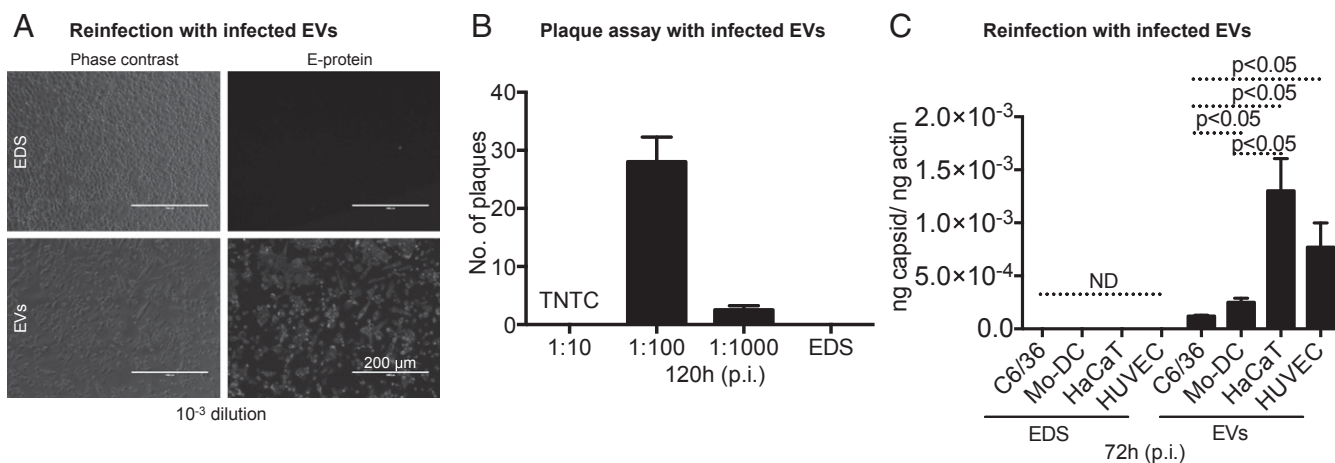


**Fig. 2.** EVs derived from mosquito cells are infectious and transmit DENV2 to both arthropod and mammalian cells. (A) Fluorescent microscopic images showing detection of E-protein in C6/36 cells infected via EVs derived from independent batch of DENV2-infected (MOI 5; 72 hpi) C6/36 cells. EDS-treated cells serve as control ( $n = 5$ ). (Scale bar, 200  $\mu\text{m}$ .) (B) Quantitative assessment of number of plaques on Vero cells treated with EVs (in different dilutions) or (EDS) fractions (as similar dilution) derived from DENV2-infected (MOI 5, 72 hpi) C6/36 cells are shown. TNTC indicates “too numerous to count” ( $n = 2$ ). (C) qRT-PCR analysis showing viral loads at 72 hpi in naïve C6/36 or mouse dendritic or human HaCaT or HUVEC cells treated with EVs or EDS fractions derived from DENV2-infected (MOI 5, 72 hpi) C6/36 cells are shown ( $n = 3$  for each cell line). ND indicates not detectable. Depending on the cells that were used, DENV2 capsid mRNA levels were normalized to mosquito, mouse, or human actin levels.

(SI Appendix, Fig. S7A and B). No detection of *hsp70* transcript (GenBank accession no. JN132154) was observed in uninfected or DENV2-infected C6/36 cell-derived EVs. Even though, expression of the other *hsp70* transcript (GenBank accession no. XM\_019672019) was clearly evident in EVs, no significant ( $P > 0.05$ ) difference was noted between uninfected or DENV2-infected groups (SI Appendix, Fig. S7C). Immunoblotting analysis showed an increased level of HSP70 in EVs isolated from DENV2-infected (MOI 5) cells at 24 hpi in comparison with 48 and 72 hpi time points and uninfected controls (SI Appendix, Fig. S7D). In addition, no differences in HSP70 levels were noted in uninfected or DENV2-infected C6/36 cell lysates at all tested time points (24, 48, and 72 hpi) and their respective uninfected controls (SI Appendix, Fig. S7D). Coomassie-stained gel images show the total protein profiles in EVs and total cell lysates (SI Appendix, Fig. S7D).

Next, we determined the role of mosquito HSP70 in EV-mediated DENV2 transmission. VER-155008 is an adenosine-derived inhibitor of the 70-kDa families of HSPs that target the ATPase binding domain (31, 32). qRT-PCR analysis showed that C6/36 cells treated (for 4 h) with VER-155008 inhibitor (at 10 and 20  $\mu\text{M}$ ), followed by infection with DENV2 (MOI 5, for 72 hpi) had significantly ( $P < 0.05$ ) reduced levels of *hsp70* (XM\_019672019) transcript levels, in comparison with the mock-(DMSO) treated group (SI Appendix, Fig. S7E). No differences were observed in XM\_019672019 levels in EVs derived from these inhibitor-treated and DENV2-infected C6/36 cells (SI Appendix, Fig. S7E). Furthermore, treatment with VER-155008 inhibitor at tested doses of 10 and 20  $\mu\text{M}$ , in comparison with the respective mock controls, showed no differences in DENV2 loads (at 72 hpi) in both total cell and EV lysates (SI Appendix, Fig. S7F). In addition, we tested the effects of VER-155008 inhibitor-treated EVs (derived from DENV2-infected, MOI 5, 72 hpi, C6/36 cells) and EDS from the same batch of preparations (SI Appendix, Fig. S7G) on naïve C6/36 cells incubated with infectious EVs for 72 hpi. No differences were found in DENV2 loads in the inhibitor-treated group compared with the respective mock controls (SI Appendix, Fig. S7G). Furthermore, we did not observe any differences in DENV2 loads of naïve C6/36 cells incubated with EDS fractions in comparison with their respective mock controls (SI Appendix, Fig. S7G). As expected, DENV2 loads in EV fractions showed significant ( $P < 0.05$ ) differences compared with the EDS fractions (SI Appendix, Fig. S7G). These data suggest the up-regulation of mosquito HSP70 as arthropod stress response during DENV2 infection, but inhibition of this critical chaperone does not regulate viral replication and transmission through EVs.

**Identification of Mosquito EV Marker Tsp29Fb, a Tetraspanin Domain-Containing Glycoprotein.** Several studies have considered proteins, such as human CD63, that are associated with membranes of intracellular vesicles as classic markers of EVs/exosomes (33–36). Lötvall et al. (17) have shown that CD63 is present on both EVs/exosomes and can thus be a marker for both large and small vesicles. CD63 belongs to the tetraspanin family of transmembrane-domain proteins (35). Using a human CD63 primary amino acid sequence (GenBank accession no. AHI151903) as a query in the VectorBase, we identified tetraspanin domain-containing mosquito orthologs in both *A. aegypti* (AAEL012532-RA) and *A. albopictus* (AALF020630-RA) and designated these orthologs as Tsp29Fb. ClustalW alignment of an *A. aegypti* Tsp29Fb amino acid sequence (SI Appendix, Fig. S8A) revealed 89% identity with *A. albopictus* Tsp29Fb and 51% identity with *Drosophila melanogaster* tetraspanin 29Fb (GenBank accession no. AAF90138). In addition, *A. aegypti* Tsp29Fb showed 28% and 27% identity (SI Appendix, Fig. S8A) with human and mouse CD63 (GenBank accession no. CAJ18387), respectively. Furthermore, the phylogenetic analysis revealed that *A. aegypti* Tsp29Fb comes within the same clade with *A. albopictus* Tsp29Fb and *D. melanogaster* tetraspanin 29Fb, whereas human and mouse CD63 counterparts form a different clade (SI Appendix, Fig. S8B). The domain analysis of

*A. aegypti* Tsp29Fb primary amino acid sequences revealed the presence of the tetraspanin domain (amino acids 15–238), four transmembrane regions (amino acids 19–41, 56–78, 90–112, 211–233), four myristoylation sites (amino acids 37–47, 76–82, 92–98, 228–234), and two glycosylation sites (amino acids 125–129, 168–172) (SI Appendix, Fig. S8C). Identification of Tsp29Fb in the mosquito genome suggests the presence of a putative EV marker in arthropods.

**DENV2 Infection Up-Regulates Tsp29Fb Levels in Mosquitoes, in EVs, and in Cells.** To understand the role of human CD63-like tetraspanin domain-containing arthropod EV marker, Tsp29Fb, we first analyzed the expression levels of this molecule. In DENV2-infected *A. aegypti* mosquitoes (in vivo), we found that *tsp29Fb* mRNA (accession no. AAEL012532-RA) loads were significantly ( $P < 0.05$ ) up-regulated at all tested time points of 24, 48, and 72 hpi, in comparison with the uninfected controls (Fig. 3A). We also tested the expression of *tsp29Fb* mRNA in Aag-2 cells, derived from *A. aegypti* mosquitoes (37). qRT-PCR analysis showed that in both Aag-2 cell-derived EVs and in cells, *tsp29Fb* (accession no. AAEL012532-RA) transcripts were up-regulated upon DENV2 infection at the tested time points (48 and 72 hpi in EVs or Aag-2 cells), compared with the uninfected controls (Fig. 3B and C). qRT-PCR analysis further revealed a significantly ( $P < 0.05$ ) higher mRNA transcript of *tsp29Fb* (accession no. AALF020630-RA) at 24 and 48 hpi in C6/36 cell-derived EVs (Fig. 3D), and at 48 and 72 hpi in whole-cell lysates (Fig. 3E). We first determined that human CD63 antibody with a large tetraspanin epitope region showed high cross-reactivity to Tsp29Fb, the arthropod homolog with greater conservation and similarity to the vertebrate CD63. Immunoblotting performed on C6/36 cell-derived EV fractions and whole-cell lysates at different time points of 24, 48, and 72 hpi, showed an increase in Tsp29Fb protein levels in DENV2-infected (MOI 5) lysates in comparison with the uninfected controls (Fig. 3F). Furthermore, these data correlated with the capsid mRNA transcript loads noted in EVs and C6/36 cell lysates (Fig. 3D and E). In addition, we also noted that an increased dose of DENV2 (with different MOI; MOI from 1 to 5) also affected Tsp29Fb loads in both EVs and total cell lysates (Fig. 3G). Densitometry analysis from EVs and total cell lysates [tested time points (48 and 72 hpi) and MOI (1 and 5) dose–response] showed the quantitative differences in Tsp29Fb levels observed between DENV2-infected and uninfected controls (SI Appendix, Fig. S9). E-protein loads increased with both the infection time course of 24, 48, and 72 hpi, and with the higher infectious doses (MOI 1–5, 72 hpi) in both DENV2-infected EVs and total cell lysates in comparison with the uninfected control (Fig. 3F and G). Total protein profiles in all four panels served as loading controls (Fig. 3F and G). These data show that Tsp29Fb is up-regulated both in vivo and in vitro upon DENV2 infection.

**Tsp29Fb, an Arthropod EV Marker, Directly Interacts with DENV2 Envelope Protein.** To characterize the role of Tsp29Fb in facilitating DENV2 infection and transmission, we analyzed if this putative arthropod EV marker directly interacts with DENV2 E-protein. Immunoprecipitation (IP) performed with highly cross-reactive human CD63 antibody and DENV2-infected (MOI 5, 72 hpi) cell-derived EVs and whole-cell lysates (suspended in modified RIPA protein lysis buffer; 150  $\mu\text{g}$  as input in each group) showed the presence of DENV2 E-protein by immunoblotting with 4G2 antibody (Fig. 3H). Direct binding of Tsp29Fb to DENV2 E-protein was enhanced in cell lysates in comparison with the EV lysates, perhaps due to the presence of enhanced Tsp29Fb protein (Fig. 3H). As expected, no E-protein signal was detected in uninfected controls processed together for IP (Fig. 3H). To exclude the possibility that direct interaction or binding of Tsp29Fb to DENV2 E-protein is not due to any E-protein contamination from EVs pelleted in PBS suspensions, we performed an independent IP assay on intact EVs suspended in PBS

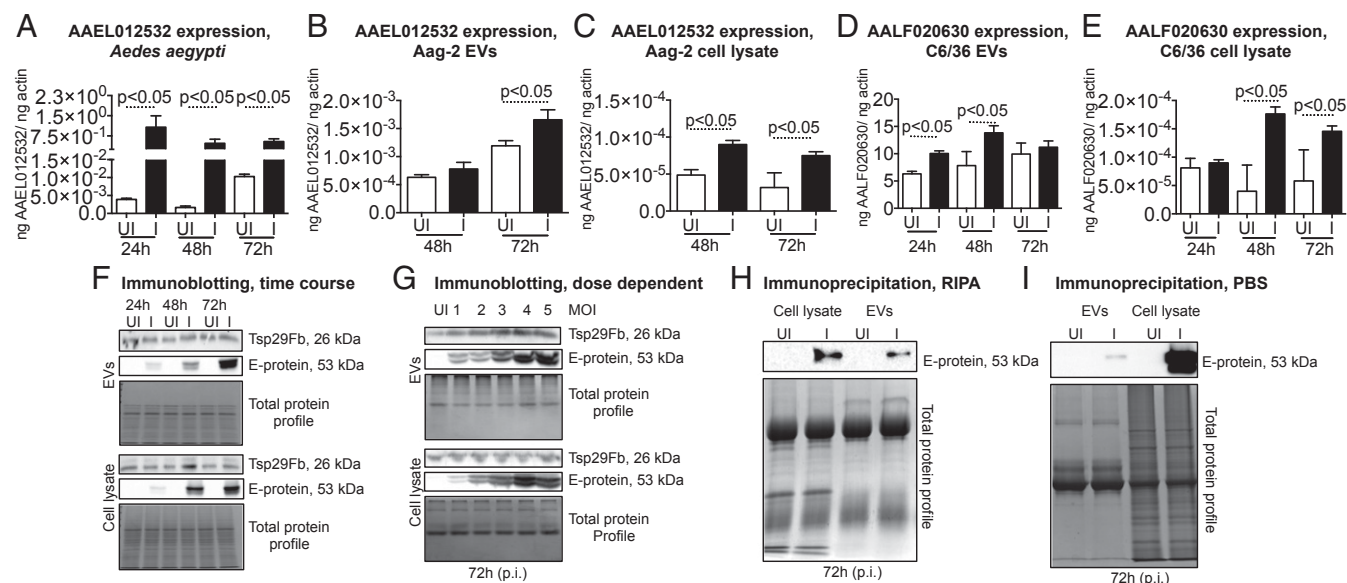


**Fig. 3.** DENV2 induces expression of Tsp29Fb, a putative EV-enriched marker on mosquito cells. (A) qRT-PCR analysis showing expression of *A. aegypti* Tsp29Fb in uninfected (UI) or DENV2-infected (I) whole mosquitoes at 24, 48, and 72 hpi ( $n = 4$ ), or in EVs (B) isolated from an uninfected (UI) or DENV2-infected (MOI 5) in vitro cell line or in Aag-2 whole-cell lysates at 48 and 72 hpi ( $n = 4$ , in both EVs or cell-lysate panels) (C). qRT-PCR analysis showing expression of *A. albopictus* Tsp29Fb ortholog in EVs (D) isolated from uninfected (UI) or DENV2-infected (MOI 5) C6/36 cells or in whole-cell lysates (E) at 24, 48, and 72 hpi ( $n = 8$ , in both EVs or cell-lysate panels). Tsp29Fb or DENV2 capsid mRNA levels were normalized to mosquito actin levels.  $P$  value determined by Student's two-tail  $t$  test is shown. (F) Immunoblotting analysis showing levels of Tsp29Fb and viral E-protein in EVs derived from uninfected (UI) or DENV2-infected (MOI 5) C6/36 cells or in whole-cell lysate at 24-, 48-, and 72-hpi time points. (G) Immunoblotting analysis showing levels of Tsp29Fb and viral E-protein in EVs derived from uninfected (UI) or DENV2-infected (MOI 5, 72 hpi) C6/36 cells or in whole-cell lysates upon DENV2 infection with different viral doses (MOI 1–5) is shown. Immunoblotting analysis of CD63 (Tsp29Fb) IP proteins in RIPA (H) or in 1 $\times$  PBS buffer (I) with 4G2 antibody showing detection of viral E-protein in EVs or whole-cells lysates derived from DENV2-infected (MOI 5, 72 hpi) C6/36 cells. Uninfected cells were used as controls in all assays. Gel images showing total protein profiles in F–I serve as loading control for respective immunoblots. Tsp29Fb and DENV2 E-protein molecular mass is indicated as kilodaltons.

instead of modified RIPA protein lysis buffer. IP of Tsp29Fb on PBS suspended intact arthropod EVs (freshly isolated) using human CD63 antibody followed by immunoblotting with 4G2 antibody again detected the precipitation of DENV2 E-protein in both mosquito cell-derived EV fractions and whole-cell lysates (we used 500  $\mu$ g as input in each group for IP with PBS suspended EV fractions) (Fig. 3I). We noted enhanced binding of Tsp29Fb with viral E-protein in cell lysates in comparison with the EV fractions (Fig. 3I) that correlated with a previous IP assay performed on EV fractions resuspended in modified RIPA buffer (Fig. 3H). Coomassie blue-stained gel images showing total protein profile of input lysates used for IP served as controls (Fig. 3H and I). Immunofluorescence merged images showed colocalization of Tsp29Fb (SI Appendix, Fig. S10A, green) with DENV2 E-protein (SI Appendix, Fig. S10A, red) in C6/36-infected cells (MOI 5, 72 hpi). Uninfected C6/36 cells and nuclei-stained (DAPI) images (along with phase-contrast) served as controls (SI Appendix, Fig. S10A). In addition, we also found that Tsp29Fb neither interacts nor coprecipitates with actin in either DENV2-infected (MOI 5, 72 hpi) EVs or total cell lysates (SI Appendix, Fig. S10B). These data served as a negative control for the direct interaction of Tsp29Fb with DENV2 E-protein (SI Appendix, Fig. S10B). We have been able to detect actin protein in both cells and EVs lysates (resuspended in RIPA buffer) used as input for the IP assay (SI Appendix, Fig. S10C). These data suggest the presence of actin in input lysates that neither interact nor coprecipitate with Tsp29Fb. Taken together, these data suggest that arthropod EV marker Tsp29Fb directly interacts with DENV2 E-protein, perhaps to facilitate infection and transmission from vector to the vertebrate host.

**Silencing or Blocking of Tsp29Fb Reduces DENV2 Infection.** We performed silencing studies, to understand the importance of Tsp29Fb in

DENV2 pathogenesis and in transmission of infectious EVs to the vertebrate host. We selected the transfection-friendly Aag-2 cells that contain proteins involved in the RNAi pathway (6, 37). First, we amplified a 252-bp fragment from an *A. aegypti* mosquito cDNA sample and cloned it into the BglII and KpnI sites of the L4440 double T7 Script II vector (38) (SI Appendix, Fig. S11A and B). Silencing of *tsp29Fb* (by transfection with double-stranded RNA) showed significantly ( $P < 0.05$ ) decreased *tsp29Fb* mRNA in Aag-2 cells in comparison with the mock-transfected group (Fig. 4A). Lower numbers of *tsp29Fb* transcripts were exported to the EVs derived from these cells (Fig. 4A). We also found that DENV2 loads (MOI 5, 24 hpi) were significantly ( $P < 0.05$ ) reduced in both EVs and Aag-2 cell lysates upon silencing of *tsp29Fb*, in comparison with the mock-transfected controls (Fig. 4B). Immunoblotting analysis revealed similar results with reduced E-protein and Tsp29Fb protein loads in both Aag-2 cell-derived EVs and total cell lysates upon treatment with *tsp29Fb-dsRNA* in comparison with the mock-treated controls (Fig. 4C). Densitometry analysis from total cell and EV lysates showed the quantitative differences in Tsp29Fb protein levels observed between the DENV2-infected (MOI 5, 24 hpi) and uninfected controls (SI Appendix, Fig. S11C). Total protein profiles shown by Coomassie-stained gel served as loading controls (Fig. 4C). Furthermore, we tested the functional-blocking effects of highly cross-reactive human CD63 antibody in mosquito cells. qRT-PCR data showed that cells treated (2 h) with either 5 or 10  $\mu$ g of human CD63 antibody, followed by infection with DENV2 (MOI 5), showed significantly ( $P < 0.05$ ) reduced viral loads (at 72 hpi) in both C6/36 cell-derived EVs (Fig. 4D) and in cells (Fig. 4E). Immunoblotting analysis revealed dramatic reduction in the DENV2 E-protein loads in both 5 and 10  $\mu$ g of CD63 antibody-treated mosquito cell-derived EVs and cell lysates, in comparison with the untreated controls (Fig. 4F). Total protein profiles shown by Coomassie-stained gels served as controls (Fig. 4F). Noticeable differences observed with CD63

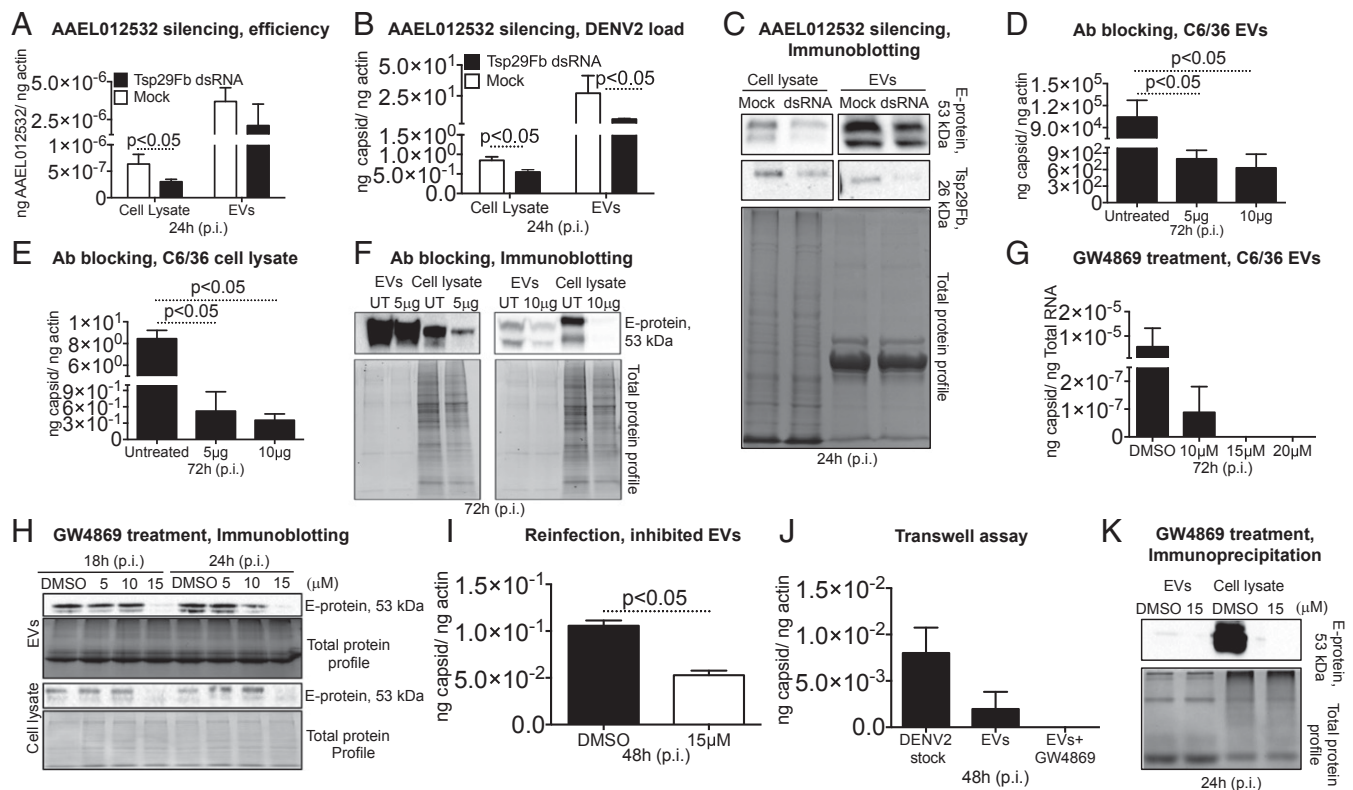


**Fig. 4.** RNAi-mediated silencing or antibody blocking of Tsp29Fb or treatment with GW4869 inhibitor affects DENV2 burden in mosquito cells and EVs. qRT-PCR analysis showing expression of *A. aegypti* Tsp29Fb to reveal silencing efficiency (A) or viral burden (B) in whole-cell lysates or EVs derived from DENV2-infected (MOI 2, 24 hpi) Aag-2 cells treated with mock or Tsp29Fb-dsRNA ( $n = 6$ ). (C) Immunoblotting analysis showing levels of *A. aegypti* Tsp29Fb or viral E-protein in whole-cell lysates or EVs derived from DENV2-infected (MOI 2, 24 hpi) Aag-2 cells treated with mock or Tsp29Fb-double-stranded RNA. qRT-PCR (D and E) ( $n = 3$ ) or immunoblotting (F) analysis showing viral burden in EVs (D and F) or whole-cell lysates (E and F) derived from DENV2-infected (MOI 5, 72 hpi) C6/36 cells treated with CD63 (Tsp29Fb) antibody at different doses (of 5 and 10  $\mu\text{g}$ ). Untreated, but DENV2-infected (MOI 2, 72 hpi) C6/36 cells were used as mock controls in D–F. qRT-PCR (G) ( $n = 4$ ) or immunoblotting (H) analysis showing viral burden in EVs (G and H) or whole-cell lysates (H) derived from DENV2-infected (MOI 2) C6/36 cells at 72 hpi (G) or at 18 or 24 hpi (H), treated with GW4869 inhibitor at different doses (of 5–20  $\mu\text{M}$ ). EVs or whole-cell lysates derived from DMSO-treated DENV2-infected C6/36 cells were used as controls in G and H. (I) qRT-PCR analysis showing viral burden in naive C6/36 cells at 48 hpi, (re-infection) upon treatment with EVs derived from DMSO- or GW4869-treated DENV2-infected (MOI 2, 72 hpi) C6/36 cells ( $n = 4$ ). (J) qRT-PCR analysis showing viral loads at 48 hpi in HUVEC cells in a transwell assay performed with C6/36 cells (in upper chamber) and naive HUVEC cells (in lower chamber) treated with EVs derived from DENV2-infected (MOI 2, 72 hpi) C6/36 cells (25  $\mu\text{L}$ , in upper chamber) for 4 h in the presence or absence of GW4869 (20  $\mu\text{M}$ ). C6/36 cells infected with DENV2 laboratory stocks with known titers were used as internal controls ( $n = 4$ ). Tsp29Fb or DENV2 capsid mRNA levels were normalized to mosquito (A, B, D, E, and I), or human (J) actin levels, but in G, DENV2 loads were normalized to total RNA. *P* value determined by Student's two-tail *t* test is shown. (K) Immunoblotting analysis of CD63 (Tsp29Fb)-IP proteins with 4G2 antibody and EVs or whole-cell lysates derived from DMSO- or GW4869-treated DENV2-infected (MOI 2, 24 hpi) C6/36 cells. Tsp29Fb and DENV2 E-protein molecular mass is indicated in kilodaltons. Coomassie-stained gel images showing total protein profiles in C, F, H, and K serve as loading control for the respective immunoblots.

antibody treatments suggest that blocking of mosquito ortholog Tsp29Fb function reduces DENV2 loads in cells and that ultimately reduces transmission of viral RNA and proteins via infectious EVs.

**GW4869 Inhibitor Reduces DENV2 Loads, Transmission, and Tsp29Fb Interactions with the Viral E-Protein.** GW4869 (dihydrochloride hydrate) is a cell-permeable but selective inhibitor for neutral sphingomyelinase (an essential enzyme required for EV production and release). Treatment of C6/36 cells with GW4869 at different concentrations (10, 15, and 20  $\mu\text{M}$ ) followed by DENV2 infection (MOI 5, 72 hpi) showed significantly ( $P < 0.05$ ) reduced capsid transcript loads in EVs, compared with the DMSO control (Fig. 4G). Similar results were obtained with immunoblotting analysis using 4G2 antibody that showed reduced levels of DENV2 E-protein at 18 and 24 hpi, and the tested concentrations (5, 10, and 15  $\mu\text{M}$ ) in both infected (MOI 5) C6/36 cell-derived EVs and cell lysates in comparison with the DMSO controls (Fig. 4H). In both mosquito cells and EVs, the reduction in E-protein loads was much affected at 24 hpi (15- $\mu\text{M}$  treatments) in comparison with the 18-hpi time point, suggesting that higher amounts

and times of incubation with GW4869 had severe effects on DENV2 infection and transmission (Fig. 4H). Total protein profiles shown by Coomassie-stained gels served as controls (Fig. 4H). Infection of naive C6/36 cells with EVs derived from DENV2-infected (MOI 5, 72 hpi) mosquito cells treated with 15  $\mu\text{M}$  of inhibitor or the DMSO-treated control group showed that treatment with GW4869 not only reduced DENV2 viral RNA replication but also transmission to naive C6/36 cells in comparison with the DMSO controls (Fig. 4I). Transwell assays performed on naive/uninfected C6/36 cells [plated on upper chambers or inserts that were infected via EVs collected from an independent batch of DENV2-infected (MOI 5, 72 hpi) C6/36 cells or infected mosquito cells treated with 20  $\mu\text{M}$  of GW4869 inhibitor] produced fresh EVs that were capable of transmigration and infecting naive HUVEC cells (plated in lower chambers) (Fig. 4J). HUVEC cells incubated with inhibitor- (20  $\mu\text{M}$ ) treated EVs showed reduced DENV2 loads (at 48 hpi) in comparison with the untreated infectious EV fractions (Fig. 4J). Infections using the DENV2 laboratory viral stocks (with known titers, we used 5 MOI) served as internal controls (Fig. 4J). Furthermore, IP performed with

CD63 antibody and lysates from DENV2-infected (MOI 5, 24 hpi) C6/36 cells treated with GW4869 inhibitor (15  $\mu$ M) or DMSO control confirmed that blocking of EV release affects the direct interaction of Tsp29Fb with DENV2 E-protein in both cells and EVs (Fig. 4K). These data further suggest that direct interaction of Tsp29Fb with E-protein is not only required for DENV2 infection and pathogenesis in the arthropod host, but is also essential for transmission of infectious EVs to the human host.

## Discussion

The modes or the molecular determinants that participate in the transmission of arthropod-borne flavivirus from the vector to the vertebrate host are not completely understood. To address this basic but very fundamental question, we explored the role of EVs in flavivirus transmission. EVs, including exosomes, have been shown as vehicles of transmission for a variety of microorganisms, and recent findings of hepatitis C virus transmission through hepatic exosomes have provided new insights into hepatitis drug discovery (19, 21, 39–41). The recent discoveries of functional RNA, miRNA, and proteins in the EVs/exosomes has increased the attention that has led to the emergence of numerous studies in identifying novel molecules present in the EVs/exosomes (12–16, 39, 42). Because of the occurrence of RNA in the EVs, we hypothesized whether arthropod EVs are also carriers of viral RNA from mosquito-borne flaviviruses. In this study we have shown the presence of a full-length DENV2 genome in EVs and that DENV2/DENV3 infectious viral RNA and proteins are also securely contained and transported to the mammalian cells through mosquito cell-derived EVs. The genome RNA of flaviviruses is single-stranded with  $\sim$ 11 kb in length that is infectious with positive polarity encoding the viral proteins required for RNA replication (43–45). Our data suggest that perhaps the full-length genomes of other serotypes of DENVs and other related flavivirus genomes are securely contained in arthropod EVs for transmission. For DENVs (serotypes 1–4), an antibody-dependent enhancement (ADE) of viral replication was noted in vitro that lead to the understanding of pathogenesis of dengue in animal models and humans (46–48). A specific range of antibody titer has been shown to enhance such viral replication (46–48). In humans, although suspected, such ADE leading to severe disease has not been shown to occur (46). Nonneutralizing antiviral proteins (i.e., the antibodies) facilitate virus entry into the host cells by binding to the Fc receptors in the plasma membrane, thereby leading to increased infectivity and ADE (49). We have previously shown that tick-borne Langat virus RNA and proteins are securely contained inside tick exosomes and that exosome-mediated Langat virus transmission to recipient cells is through receptor-dependent endocytosis that requires clathrin (19). We assume that the presence of DENV2/DENV3 RNA and proteins inside EVs perhaps escape the viral check points by host-neutralizing or nonneutralizing antibodies. This could allow enhanced fusion of EVs on recipient cells through clathrin-dependent receptor-mediated endocytosis and thereby facilitate infection. We assume that EV-mediated transmission may result in ADE of DENV replication.

In our multiple cryo-EM analyses, we did not find the presence of intact virions/viral particles inside or outside of the EVs or in the PBS suspensions, as we have used 72 hpi as the time point for analysis. To make virus preparations, concentrated supernatants from longer times of infection (7–14 dpi) with higher titers ( $10^9$  to  $10^{12}$  PFU/mL) and centrifugal forces of  $200,000 \times g$  have been used (50) that are not similar to the one used in our EV preparations (*SI Appendix, Fig. S2*). To avoid longer incubation days and peak of infection resulting in cell death, we considered performing all experiments at 72 hpi; however, longer times of infection (days 7–14) may reveal differences in the DENV2-infected group. Mosquito cell-derived EVs were found to be of heterogeneous

population, varying from sizes of 30–250 nm; however, fewer of them were with sizes of 250–350 nm and could be considered as EVs. The quantitative analysis of the cryo-EM data suggested a smaller number of large-size EVs in the DENV2-infected (72 hpi) group compared with the number of EVs from the uninfected group. In addition, the DENV2-infected smaller EVs/exosomes of 30- to 100-nm size were abundantly present, suggesting that viral RNA and proteins are perhaps more secured in smaller EVs due to greater integrity/stability during release from cells or during fusion with recipient cells.

EVs isolated from the density gradient method that also resulted in purified EV preparations (18), showed the presence of HSP70, the EV-enriched protein. Detection of DENV2 E-protein in the same fraction suggested that perhaps these are EVs/exosomes, with size ranges of 50–100 nm that were analyzed as the highest percentages with quantitative estimation from cryo-EM images. EV quantification largely relies on their physical characteristics or properties—such as size, mass, and density—or the membrane proteins presented on their surface as cargo. For other quantification methods, such as Nanodrop or Nanosight, high concentrations of EVs are required and the results are mostly variable (51, 52). Increase in the presence of a specific EV biomarker has been correlated with a general increase in vesicle secretion, or rather with an increase in biomarker density on the surface of vesicles (51, 52). However, the differential cargo loading on EVs each time would perhaps suggest variability in using biomarkers for quantification. The reference to the total protein concentration (determined by the BCA method) each time has given us very reliable and consistent results on the routine isolation of EVs. The abundant amount of E-protein in arthropod EVs in comparison with the cell lysates suggests the higher packaging of E-protein for transmission to human and other vertebrate host cells. In addition, we assume that an abundant amount of viral RNA and proteins inside cells may randomly get trafficked into EVs. We hypothesize that dissemination of infectious EVs within mosquitoes from hemolymph to the salivary glands and subsequently to the mosquito saliva may efficiently facilitate the transmission of the infectious viral RNA and proteins to the vertebrate host through an infected arthropod bite site during blood feeding.

The observation of no differences in the viral loads in 4G2 antibody-beads binding assay suggests that E-protein is contained inside the EVs. If E-protein or viral particles are present outside the EVs as contaminants, the 4G2 antibody could bind E-protein, resulting in lower viral loads in comparison with the isotype antibody-treated or untreated controls. Treatment of DENV2 viral stocks with 4G2 antibody showed binding of surface-exposed E-protein, but not in the EV group, as E-protein was contained inside EVs and hence was unavailable to bind 4G2 antibody. These differences in 4G2 antibody binding to E-protein suggest that E-protein is securely contained inside the arthropod EVs. RNaseA-treatment assays were in agreement with the antibody-beads binding assay that further suggests no RNA binding outside of EVs or no availability of free viral RNA being presented outside of the EVs. If viral RNA was present in PBS suspensions containing EVs, we should expect an enhanced viral load in samples not treated with RNaseA in comparison with the treated group. These data are further supported by native-PAGE immunostaining with 4G2 antibody and ELISAs that showed more intense signal in the Triton X-100-treated group in comparison with the untreated controls. Native-PAGE analysis indicated detection of either higher complexes of E-protein as dimer or oligomers or perhaps the presence of viral polyprotein (at higher molecular mass) under nonreducing conditions and in the native state. The observation of lower molecular mass of E-protein (as detected by 4G2 antibody) upon Triton X-100 treatment suggests lysis of EVs and breakdown of higher molecular mass of E-proteins. In addition, the observation of no detection of fluorescent signal (with 4G2 antibody), no plaque

formation, and no amplification of capsid mRNA transcripts in EV-free or EDS further suggests that the preparations were clean and contained viral RNA and proteins inside the EVs. Infection of different cell lines (mouse and human), including mosquito cells with infectious arthropod-derived EVs, suggest that the viral RNA and proteins are contained inside the EVs that are capable of transmission and replication in recipient cells.

HSPs include both constitutive and stress-inducible members that interact with native and denatured proteins to facilitate the proper folding of native proteins or refolding of the denatured proteins (27, 28). In addition to their essential roles in intracellular trafficking, they also prevent the cytotoxic aggregation or misfoldings of the aberrantly folded proteins (27, 28). HSPs have been shown to play diverse behavioral, biochemical, and physiological roles in insects and one of the most essential cellular responses is a rapid increase in expression of HSPs upon stress (30). HSP70 is the most widely studied responder to heat and other stresses and at least 12 HSP proteins have been shown to abundantly increase in response to heat/temperature (53–55). The levels of mosquito HSP70s have been documented to increase during several environmental stresses, and several *hsp* genes are up-regulated following a blood meal in mosquitoes (53–55). Up-regulation of HSP70 homologs upon DENV2 infection suggested a protective role of this molecule during DENV2-induced stress. The presence of only one isoform (XM\_019672019) of HSP70 in EVs suggests the importance of this molecule possibly in the chaperone activity inside EVs. The observation of no effect on DENV2 loads in EVs upon treatment with VER-155008 inhibitor suggests that HSP70 is perhaps not required for DENV2 replication in cells and release into EVs. In addition, the observation of no differences in the DENV2 loads in naïve C6/36 cells upon treatment with infectious EVs [derived from HSP70-inhibitor-treated and DENV2-infected (MOI 5, 72 hpi) C6/36 cells] suggests that HSP70 may not be required for EV-mediated transmission of DENV2 RNA and proteins.

Identification of the transmembrane/tetraspanin domain-containing glycoprotein Tsp29Fb from *A. aegypti* mosquito cells and EVs derived from both *A. aegypti* (Aag-2) and *A. albopictus* (C6/36) cells indicated the presence of this molecule in both species. Up-regulation of Tsp29Fb upon DENV2 infection at both mRNA and protein levels and in both cells and EVs lysates confirmed the importance of this molecule in mediating DENV2 infection and transmission of infectious viral RNA and proteins via EVs. Identification and characterization of this arthropod EV-enriched marker provides information on the molecular determinants that facilitate transmission of DENV2 from vector to the vertebrate host. Furthermore, the direct interaction and coassociation of Tsp29Fb with DENV2 E-protein suggests a potential role of this molecule in mediating DENV2 replication and transmission via the arthropod endo-exosomal pathway. The enriched signal for E-protein in both IP assays could be because of the enhanced production and more availability of Tsp29Fb to

physically bind with DENV2 E-protein in cells compared with the EV fractions. Trafficking of other required cargo may also limit the loading of more Tsp29Fb in DENV2-infected EVs (16, 22, 36, 56, 57). Silencing of Tsp29Fb in cells showed a significant reduction in DENV2 cellular loads and significantly reduced export of the viral RNA and E-protein in EVs. Furthermore, functional blocking of Tsp29Fb clearly showed reduced DENV2 loads in both EVs and cells. These data clearly showed the prominence of this arthropod molecule in mediating DENV2 replication, release, and transmission via EVs.

The use of exosome release inhibitor GW4869 at lower tested doses of 10–20  $\mu$ M further confirmed that DENV2 transmission is mediated via EV release. The inhibitor treatment dramatically decreased the DENV2 capsid mRNA and E-protein. In addition, blocking of EVs/exosome release by GW4869 reduced the infectious viral RNA and protein transport, thereby dramatically blocking the transmission to human blood endothelial cells. The direct interaction of the viral E-protein with Tsp29Fb was also affected by treatment with GW4869, suggesting a role for this arthropod marker in the EVs/exosome release pathway. It would be an interesting future avenue to investigate the mechanism of this viral inhibition through blocking the release of EVs from arthropod saliva. The finding that inhibition of EVs/exosome release upon GW4869 treatment in arthropod cells suggests the presence of neutral sphingomyelinase in mosquitoes. Overall, our study suggests that inhibition of arthropod tetraspanin domain-containing glycoprotein Tsp29Fb or inhibition of EVs/exosome release through the GW4869 inhibitor are both potential therapeutics to block transmission of DENV2 and perhaps other mosquito-borne flaviviruses.

## Materials and Methods

*A. albopictus* (C6/36 cells) and the African Green Monkey kidney Vero cell line were obtained from ATCC. The *Aedes aegypti* (Aag-2) cell line was obtained from T.M.C.'s laboratory. Mouse Mo-DCs, HaCaT cells, and HUVECs were obtained from the Piotr Kraj, Loree Heller, and John Catravas laboratories, respectively, Old Dominion University, Norfolk, Virginia. DENV2 El Salvador strain (TVP2176) was obtained from John F. Anderson, Connecticut Agricultural Experiment Station, New Haven, Connecticut. DENV3 (DENV-3/US/BID-V1619/2005) or the DENV2 New Guinea C strains were obtained from BEI Resources. Detailed materials and methods can be found in *SI Appendix*.

**ACKNOWLEDGMENTS.** We thank Drs. Michel Ledizet (for 4G2 monoclonal antibody), John Catravas and Ms. Betsy Gregory (for providing growing human umbilical vein endothelial cells and required cell culture media), and Dr. John F. Anderson [for the generous gift of wild-type DENV2 El Salvador strain (TVP2176)]. H.S. thanks the kind support from BEI Resources. The following reagents were obtained through BEI Resources, National Institute of Allergy and Infectious Diseases, NIH: (i) monoclonal anti-Flavivirus group antigen, clone D1-4G2-4-15 (produced in vitro), NR-50327; (ii) dengue virus type 3, DENV-3/US/BID-V1619/2005, NR-43283; (iii) monoclonal anti-dengue virus type 3 envelope protein, clone E2 (produced in vitro), NR-15511. This work was supported by start-up funds from Old Dominion University (to H.S.).

- Mukhopadhyay S, Kuhn RJ, Rossmann MG (2005) A structural perspective of the flavivirus life cycle. *Nat Rev Microbiol* 3:13–22.
- Valderrama A, Díaz Y, López-Vergés S (2017) Interaction of flavivirus with their mosquito vectors and their impact on the human health in the Americas. *Biochem Biophys Res Commun* 492:541–547.
- Neelakanta G, Sultana H (2015) Transmission-blocking vaccines: Focus on anti-vector vaccines against tick-borne diseases. *Arch Immunol Ther Exp (Warsz)* 63:169–179.
- Choumet V, Despres P (2015) Dengue and other flavivirus infections. *Rev Sci Tech* 34: 473–478, 467–472.
- Li L, et al. (2008) The flavivirus precursor membrane-envelope protein complex: Structure and maturation. *Science* 319:1830–1834.
- Olagnier D, et al. (2016) Dengue virus immunopathogenesis: Lessons applicable to the emergence of Zika virus. *J Mol Biol* 428:3429–3448.
- Diamond MS, Pierson TC (2015) Molecular insight into dengue virus pathogenesis and its implications for disease control. *Cell* 162:488–492.
- Murrell S, Wu SC, Butler M (2011) Review of dengue virus and the development of a vaccine. *Biotechnol Adv* 29:239–247.
- Webster DP, Farrar J, Rowland-Jones S (2009) Progress towards a dengue vaccine. *Lancet Infect Dis* 9:678–687.
- Sultana H, et al. (2009) Fusion loop peptide of the West Nile virus envelope protein is essential for pathogenesis and is recognized by a therapeutic cross-reactive human monoclonal antibody. *J Immunol* 183:650–660.
- Alvarez ML, Khosroheidari M, Kanchi Ravi R, DiStefano JK (2012) Comparison of protein, microRNA, and mRNA yields using different methods of urinary exosome isolation for the discovery of kidney disease biomarkers. *Kidney Int* 82:1024–1032.
- Ludwig AK, Giebel B (2012) Exosomes: Small vesicles participating in intercellular communication. *Int J Biochem Cell Biol* 44:11–15.
- Colombo M, Raposo G, Théry C (2014) Biogenesis, secretion, and intercellular interactions of exosomes and other extracellular vesicles. *Annu Rev Cell Dev Biol* 30: 255–289.
- Théry C (2011) Exosomes: Secreted vesicles and intercellular communications. *F1000 Biol Rep* 3:15.
- Théry C, Zitvogel L, Amigorena S (2002) Exosomes: Composition, biogenesis and function. *Nat Rev Immunol* 2:569–579.

16. Théry C, et al. (2001) Proteomic analysis of dendritic cell-derived exosomes: A secreted subcellular compartment distinct from apoptotic vesicles. *J Immunol* 166:7309–7318.
17. Lötvall J, et al. (2014) Minimal experimental requirements for definition of extracellular vesicles and their functions: A position statement from the International Society for Extracellular Vesicles. *J Extracell Vesicles* 3:26913.
18. Tauro BJ, et al. (2012) Comparison of ultracentrifugation, density gradient separation, and immunoaffinity capture methods for isolating human colon cancer cell line LIM1863-derived exosomes. *Methods* 56:293–304.
19. Zhou W, et al. (2018) Exosomes serve as novel modes of tick-borne flavivirus transmission from arthropod to human cells and facilitates dissemination of viral RNA and proteins to the vertebrate neuronal cells. *PLoS Pathog* 14:e1006764.
20. Cvjetkovic A, Lötvall J, Lässer C (2014) The influence of rotor type and centrifugation time on the yield and purity of extracellular vesicles. *J Extracell Vesicles* 3:23111.
21. Dreux M, et al. (2012) Short-range exosomal transfer of viral RNA from infected cells to plasmacytoid dendritic cells triggers innate immunity. *Cell Host Microbe* 12:558–570.
22. Schageman J, et al. (2013) The complete exosome workflow solution: From isolation to characterization of RNA cargo. *BioMed Res Int* 2013:253957.
23. Thery C, Amigorena S, Raposo G, Clayton A (2006) Isolation and characterization of exosomes from cell culture supernatants and biological fluids. *Curr Protoc Cell Biol* Chapter 3:Unit 3.22.
24. Cousin J (2005) Cell biology: The ins and outs of exosomes. *Science* 308:1862–1863.
25. Février B, Raposo G (2004) Exosomes: Endosomal-derived vesicles shipping extracellular messages. *Curr Opin Cell Biol* 16:415–421.
26. Keller S, Sanderson MP, Stoeck A, Altevogt P (2006) Exosomes: From biogenesis and secretion to biological function. *Immunol Lett* 107:102–108.
27. Lancaster GI, Febbraio MA (2005) Exosome-dependent trafficking of HSP70: A novel secretory pathway for cellular stress proteins. *J Biol Chem* 280:23349–23355.
28. Takeuchi T, et al. (2015) Intercellular chaperone transmission via exosomes contributes to maintenance of protein homeostasis at the organismal level. *Proc Natl Acad Sci USA* 112:E2497–E2506.
29. Gross TL, Myles KM, Adelman ZN (2009) Identification and characterization of heat shock 70 genes in *Aedes aegypti* (Diptera: Culicidae). *J Med Entomol* 46:496–504.
30. Benoit JB, et al. (2011) Drinking a hot blood meal elicits a protective heat shock response in mosquitoes. *Proc Natl Acad Sci USA* 108:8026–8029.
31. Massey AJ, et al. (2010) A novel, small molecule inhibitor of Hsc70/Hsp70 potentiates Hsp90 inhibitor induced apoptosis in HCT116 colon carcinoma cells. *Cancer Chemother Pharmacol* 66:535–545.
32. Wen W, Liu W, Shao Y, Chen L (2014) VER-155008, a small molecule inhibitor of HSP70 with potent anti-cancer activity on lung cancer cell lines. *Exp Biol Med (Maywood)* 239:638–645.
33. Halova I, Draber P (2016) Tetraspanins and transmembrane adaptor proteins as plasma membrane organizers-mast cell case. *Front Cell Dev Biol* 4:43.
34. Metzelaar MJ, Schuurman HJ, Heijnen HF, Sixma JJ, Nieuwenhuis HK (1991) Biochemical and immunohistochemical characteristics of CD62 and CD63 monoclonal antibodies. Expression of GMP-140 and LIMP-CD63 (CD63 antigen) in human lymphoid tissues. *Virchows Arch B Cell Pathol Incl Mol Pathol* 61:269–277.
35. Metzelaar MJ, et al. (1991) CD63 antigen. A novel lysosomal membrane glycoprotein, cloned by a screening procedure for intracellular antigens in eukaryotic cells. *J Biol Chem* 266:3239–3245.
36. Pols MS, Klumperman J (2009) Trafficking and function of the tetraspanin CD63. *Exp Cell Res* 315:1584–1592.
37. Barletta AB, Silva MC, Sorgine MH (2012) Validation of *Aedes aegypti* Aag-2 cells as a model for insect immune studies. *Parasit Vectors* 5:148.
38. Sultana H, et al. (2010) Anaplasma phagocytophilum induces actin phosphorylation to selectively regulate gene transcription in *Ixodes scapularis* ticks. *J Exp Med* 207:1727–1743.
39. Bobrie A, Colombo M, Raposo G, Théry C (2011) Exosome secretion: Molecular mechanisms and roles in immune responses. *Traffic* 12:1659–1668.
40. Ohno S, Ishikawa A, Kuroda M (2013) Roles of exosomes and microvesicles in disease pathogenesis. *Adv Drug Deliv Rev* 65:398–401.
41. Apte-Sengupta S, Sirohi D, Kuhn RJ (2014) Immature dendritic cell-derived exosomes can mediate HIV-1 trans infection. *Proc Natl Acad Sci USA* 103:738–743.
42. Raposo G, Stoorvogel W (2013) Extracellular vesicles: Exosomes, microvesicles, and friends. *J Cell Biol* 200:373–383.
43. Apte-Sengupta S, Sirohi D, Kuhn RJ (2014) Coupling of replication and assembly in flaviviruses. *Curr Opin Virol* 9:134–142.
44. Gritsun DJ, Jones IM, Gould EA, Gritsun TS (2014) Molecular archaeology of Flaviviridae untranslated regions: Duplicated RNA structures in the replication enhancer of flaviviruses and pestiviruses emerged via convergent evolution. *PLoS One* 9:e92056.
45. Kuno G (2007) Host range specificity of flaviviruses: Correlation with in vitro replication. *J Med Entomol* 44:93–101.
46. Katzelnick LC, et al. (2017) Antibody-dependent enhancement of severe dengue disease in humans. *Science* 358:929–932.
47. Flipse J, et al. (2016) Antibody-dependent enhancement of dengue virus infection in primary human macrophages; balancing higher fusion against antiviral responses. *Sci Rep* 6:29201.
48. Goncalves AP, Engle RE, St Claire M, Purcell RH, Lai CJ (2007) Monoclonal antibody-mediated enhancement of dengue virus infection in vitro and in vivo and strategies for prevention. *Proc Natl Acad Sci USA* 104:9422–9427.
49. Guzman MG, Vazquez S (2010) The complexity of antibody-dependent enhancement of dengue virus infection. *Viruses* 2:2649–2662.
50. Fragnoud R, et al. (2015) Differential proteomic analysis of virus-enriched fractions obtained from plasma pools of patients with dengue fever or severe dengue. *BMC Infect Dis* 15:518.
51. Chia BS, Low YP, Wang Q, Li P, Gao Z (2017) Advances in exosome quantification techniques. *Trends Analyt Chem* 86:93–106.
52. Rupert DLM, Claudio V, Lässer C, Bally M (2017) Methods for the physical characterization and quantification of extracellular vesicles in biological samples. *Biochim Biophys Acta* 1861:3164–3179.
53. Benoit JB, Lopez-Martinez G, Phillips ZP, Patrick KR, Denlinger DL (2010) Heat shock proteins contribute to mosquito dehydration tolerance. *J Insect Physiol* 56:151–156.
54. Sanders HR, Evans AM, Ross LS, Gill SS (2003) Blood meal induces global changes in midgut gene expression in the disease vector, *Aedes aegypti*. *Insect Biochem Mol Biol* 33:1105–1122.
55. Marinotti O, Nguyen QK, Calvo E, James AA, Ribeiro JM (2005) Microarray analysis of genes showing variable expression following a blood meal in *Anopheles gambiae*. *Insect Mol Biol* 14:365–373.
56. Schey KL, Luther JM, Rose KL (2015) Proteomics characterization of exosome cargo. *Methods* 87:75–82.
57. Villarroya-Beltrí C, Baixauli F, Gutiérrez-Vázquez C, Sánchez-Madrid F, Mittelbrunn M (2014) Sorting it out: Regulation of exosome loading. *Semin Cancer Biol* 28:3–13.